THE JOURNAL OF PHYSICAL CHEMISTRY C
A JOURNAL OF THE AMERICAN CHEMICAL SOCIETY

pubs.acs.org/JPCC

Article

Influence of Charged Site Density on Local Electric Fields and Polar Solvent Organization at Oxide Interfaces

Somaiyeh Dadashi, Shyam Parshotam, Bijoya Mandal, Benjamin Rehl, Julianne M. Gibbs,* and Eric Borguet*

Cite This: https://doi.org/10.1021/acs.jpcc.4c00306

Read Online

ACCESS | Metrics & More | Article Recommendations | Supporting Information

ABSTRACT: The characteristics of oxide surfaces such as their hydroxyl density, the associated acid−base chemistry, and the resulting surface charge play a crucial role in modulating the solvent organization and electrostatics at interfaces found in chemical and environmental processes. Here, the nitrile mode of acetonitrile, a neutral Stark-active molecule, is used to probe the local electric fields and solvent organization that result from surface charge at the α-Al_2O_3(0001)/aqueous and SiO_2/aqueous interfaces using vibrational sum frequency generation (vSFG). The vSFG response in the C≡N stretch region for H_2O−acetonitrile mixtures displays an asymmetric line shape and unique pH-dependent behavior, which we attributed to interference with the H_2O combination (bend + libration). Stark spectroscopy results at both interfaces reveal that the density of surface hydroxyl groups influences the magnitude of the local electric field experienced by acetonitrile. While the nitrile group of acetonitrile probes single-point charges at the SiO_2 surface at pH 6−11, the local electric field sampled by the nitrile group at the Al_2O_3 interface is impacted by multiple charged hydroxyl sites at elevated pH. These findings highlight the influence of inhomogeneous surface-charging behavior on interfacial solvent structure and local electric fields.

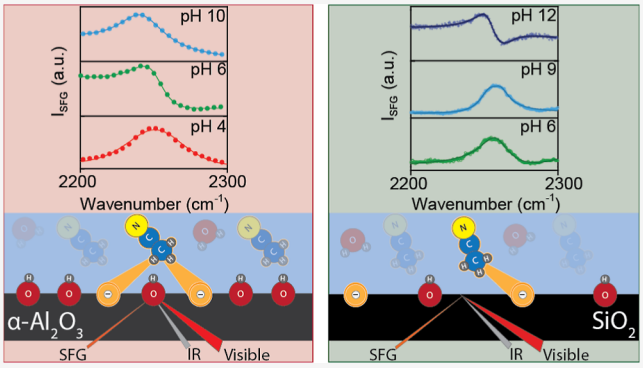

INTRODUCTION

Understanding the local electric fields and structure of polar solvents at charged oxide surfaces, such as α-Al_2O_3 and SiO_2, is important since they play a key role in chemical and environmental processes.[1−3] A practical example of a polar solvent interacting with an oxide surface can be found in high-performance liquid chromatography (HPLC) that can use α-Al_2O_3 or SiO_2 as stationary phases and water−acetonitrile mixtures as the mobile phase.[4−6] The HPLC separation process is impacted by the properties of both the mobile phase and the solid phase as well as the interaction between the solid and solvent.[4−6] The pH of the mobile phase influences the charging behavior of the solid phase.[7,8] Additionally, the break in the symmetry at an interface leads to the solvent's molecular arrangement being different from the bulk.[9] As a result, the surface charge density, the local potential, and the resulting solvent structure may affect the adsorption properties of the oxide surfaces.[10] For example, acetonitrile at SiO_2 surfaces has been found to organize as a bilayer even in the presence of H_2O, due to the hydrophobic interactions between the methyl groups.[11−17] Thus, understanding the local structure of polar solvents at the charged surface is essential since it affects interfacial chemistry, e.g., heterogeneous catalysis and electrochemistry.[18]

Even though silica and alumina surfaces are terminated by OH groups, there are several differences between them such as the point of zero charge (PZC), the density of the surface hydroxyl groups, and their acid−base chemistry.[18] The PZC of the SiO_2 surface occurs at pH ≈ 2−4 providing access to neutral and negatively charged interfaces in the pH range typically used in separation,[19] while the α-Al_2O_3(0001) has a PZC between pH ≈ 6 and 8 and allows for the positive surface to be probed at pH < 6 in addition to a neutral or negatively charged surface (above pH < 7−8).[20,21] Furthermore, the surface of the α-Al_2O_3(0001) is covered with a high density of AlOH groups (~15 OH groups/nm^2),[1,22] while the surface of SiO_2 has a lower density of surface hydroxyl groups (~5 OH groups/nm^2).[23,24]

Differences between the two oxides also result from the unique acid−base chemistry at the surface. For the SiO_2, previous work has proposed the existence of two pK_as, based on experimental second harmonic generation measurements,

Received: January 15, 2024
Revised: April 23, 2024
Accepted: April 24, 2024

and it is indicated that the pK_a of 19% of the silanol groups is 4.5, while the remaining 81% of acidic silanols exhibit a pK_a of 8.5.[23,25] This distribution appears to depend on the aqueous composition[26] and sample history.[27] The pK_a of Al_2O_3 is still a subject of debate. Using the BLYP functional, the pK_a value of the hydroxyl group on the alumina (0001) interface is reported as 16.6 by one molecular dynamics study,[28] whereas experimental potentiometric titrations report the pK_a of Al_2OH as 12.5.[29] Hence, the difference between Al_2O_3 and SiO_2 surfaces can be utilized to investigate how the organization and local electrostatics of solvents on charged oxide surfaces may vary since the surfaces have different densities of surface hydroxyl groups and different acid−base behavior.

At the α-Al_2O_3(0001) and SiO_2 surfaces, varying the pH of the bulk solvent can induce the protonation or deprotonation of surface hydroxyl groups, thereby changing the surface charge density and generating an electric field.[1] For the silica/aqueous interface, a significant increase in total surface potential and surface charge density has been observed upon increasing the pH from near neutral to pH 10 or above.[30,31] Moreover, the average static electric field present in the Stern layer at pH 10 with 10 mM NaCl electrolyte to be −4.1 MV/cm based on calculations from the reported surface charge densities, interfacial potentials, and Stern layer thickness at pH 10.[31] Yet the charge distribution on insulating oxide surfaces is heterogeneous, contrary to metal and semiconductor electrodes where the charge is homogeneously and uniformly distributed.[32,33] The surface charge density, the local potential, and the resulting solvent structure may affect the adsorption properties of the oxide surfaces.[10] However, the local potential (or local electric field) near charged sites on many oxides has not been measured.

A common approach in probing the local electric field from a charged interface is vibrational Stark effect spectroscopy (VSES).[34−37] For example, VSES has been used for the investigation of charge accumulation at electrochemical surfaces using the Stark shift of ionic liquids in the presence of an external electric field.[38] VSES correlates the vibrational frequency shift, due to changes in the vibrational energy-level spacing of probe molecules, e.g., nitrile, azide, and carbonyl groups including neutral Stark-active molecules, from the presence of a local static electric field.[39−41] In particular, the sensitivity of the nitrile mode to the nature of the local environment makes acetonitrile a useful neutral Stark-active molecule.

Previous spectroscopic measurements, including vibrational sum frequency generation (vSFG), have used acetonitrile to study solvent organization at metal electrode surfaces at different applied potentials.[42−45] In the inner Helmholtz layer, which corresponds to the specifically adsorbed and partially solvated ions, the population of the ordered acetonitrile molecules dominates when the metal is positively charged (+400 to +1200 mV vs. Ag/AgCl), with the C≡N group directed toward the metal.[45] At smaller/more negative potentials (+400 to −200 mV), the orientation of the acetonitrile flips, with the CH_3 group pointing toward the surface.[45] At even more negative potentials −200 to −800 mV (vs Ag/AgCl), water displaces acetonitrile and is present with the oxygen end pointing toward the metal.[45] These SFG results of water−acetonitrile mixtures at the metal electrode surfaces yields a model of the inner Helmholtz layer composition and how it relates to potential and surface charge variations.[45]

At the SiO_2 surface, the organization of acetonitrile has been found to resemble a supported bilayer even in the presence of H_2O,[12,16,46] due to the hydrophobic interactions between the methyl groups.[16,47,48] The influence of surface charge on the organization of H_2O−acetonitrile mixtures at silica surfaces has been investigated via the vSFG response of the CH stretching modes of acetonitrile.[16] Rehl et al. found that moving the solution from neutral to basic conditions reduced the number density of interfacial acetonitrile molecules disrupting an acetonitrile-rich layer near the interface, which was attributed to the magnitude of the external electric field generated from the deprotonation of surface SiOH sites at higher pH.[16] This provides the opportunity to utilize the C≡N mode of acetonitrile, a neutral Stark-active molecule, to determine the magnitude of local electric fields influenced by the density and the charge of the hydroxyl groups.

In this work, we hypothesize that the organization and the local electric field experienced by the solvent are influenced by the oxide surface charge, which is controlled by the acidic and basic properties of the surface as well as the surface site density.[46] We tested this hypothesis by investigating H_2O−acetonitrile mixtures at the α-Al_2O_3(0001) and SiO_2 interfaces as a function of pH with vSFG in the nitrile stretching region of acetonitrile. Qualitatively, under basic conditions, the vSFG spectra show asymmetry which we interpret as an interference of the H_2O combination (bend + libration) band with the nitrile stretch of acetonitrile. For α-Al_2O_3(0001), this asymmetry is observed when the surface is negatively charged. However, at acidic pH, where the α-Al_2O_3(0001) surface is positively charged and the polar −C≡N head of acetonitrile is expected to be directed toward the solid surface, the asymmetric pattern is not observed. For SiO_2, the presence of this combination band becomes evident only beyond the second pK_a of silanol sites (>pH 9). After accounting for this asymmetry in our spectral fitting, we determined the local electric field at positively (4.3 MV/cm: pH 4) and negatively (−16 MV/cm: pH 10) charged sites at the α-Al_2O_3(0001) surface as well as at the negatively (∼−3 MV/cm: pH 6 to 9 to 12) charged sites at the SiO_2 surfaces with respect to neutral sites (set to be ∼0 MV/cm) using the vibrational Stark shift of the nitrile mode of the acetonitrile. We find that the negatively charged sites at the α-Al_2O_3(0001) surface exhibit a very pH-dependent local electric field that at pH 10 is significantly greater than that of the SiO_2 surface. This stronger electric field can be correlated with the greater density of deprotonated sites on α-Al_2O_3(0001) owing to its intrinsic greater density of surface hydroxyl groups. In contrast, the SiO_2 does not exhibit a pH-dependent increase in the local electric field probed by the acetonitrile despite the increase in surface charge density and average surface potential expected over this pH range. These results suggest that the heterogeneity of sites on oxides can lead to local electric fields that do not increase in magnitude as the surface becomes more negatively charged. However, at a high enough surface charge density like that of α-Al_2O_3(0001), individual acetonitrile molecules sample a local field stemming from multiple charged sites. For Al_2O_3, this increase in surface charge density and local field correlates with an increase in net ordering of the interfacial acetonitrile. For SiO_2, there is an increase in vSFG intensity, interpreted as enhanced interfacial solvent order, with increasing pH. At higher pH (∼10) the vSFG intensity drops, consistent with our earlier work.[16]

https://doi.org/10.1021/acs.jpcc.4c00306
J. Phys. Chem. C XXXX, XXX, XXX−XXX

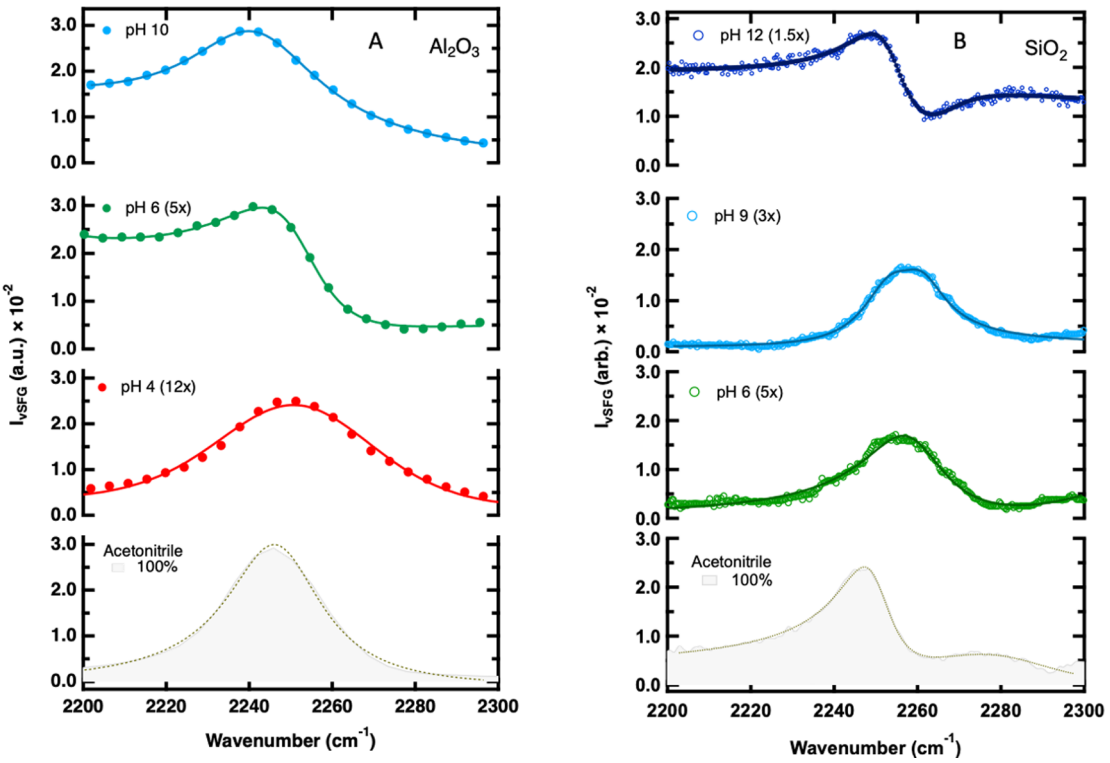

Figure 1. vSFG spectra of H_2O−acetonitrile solutions in the C≡N stretch region using the PPP polarization combination. (A) α-Al_2O_3(0001) interface at pH 4, 6, and 10 and (B) SiO_2 interface at pH 6, 9, and 12. The vSFG spectra were fit using three Lorentzian oscillators for pH 6 and 10 of α-Al_2O_3(0001) and 12 of the SiO_2. Only two Lorentzian oscillators were required for pH 4 of α-Al_2O_3(0001) and pH 6 and 9 of SiO_2 (solid lines). For the 100% acetonitrile, two Lorentzian functions are used for the SiO_2 (gray dashed) and one Lorentzian for the α-Al_2O_3(0001) (gray dashed). The details and tabulated fit parameter values can be found in the Supporting Information, Tables S1 and S2. The response for 100% acetonitrile is shown in gray at the bottom of each panel. The blue and the red arrows represent the blue shift and the red shift with respect to the frequency of the neutral site (discussed below).

EXPERIMENTAL SECTION

The vSFG experiments were carried out at the α-Al_2O_3(0001) and the SiO_2 interfaces at Temple University and the University of Alberta, respectively. Details of sample preparation, optical setup, and spectrum normalization and other information (Figure S1) can be found in the Supporting Information.

RESULTS AND DISCUSSION

To investigate the impact of the surface charge density on H_2O−acetonitrile organization at charged oxide interfaces, we performed vSFG measurements as a function of bulk solvent pH. In addition to pure acetonitrile, 50/50% and 60/40% mixtures of H_2O and acetonitrile were used for the measurements at the α-Al_2O_3(0001) and the SiO_2 surfaces, respectively. The latter ratio for the SiO_2 was chosen to maintain experimental consistency with previous studies conducted on the CH stretch of acetonitrile.[16]

The vSFG spectral shape in the C≡N stretching region of the acetonitrile measured in PPP polarization combinations [P-polarized SFG, P-polarized visible, and P-polarized infrared (IR)] shows a different trend for the neat acetonitrile and H_2O−acetonitrile mixtures at different bulk pH values at both interfaces (Figure 1A,B). These spectra of acetonitrile in the C≡N stretch region are similar to previous studies at neutral solid/liquid interfaces in that a feature is observed at 2250−2260 cm^{-1}.[49] However, the Fermi resonance peak, which arises from the coupling between the C≡N stretch and the combination band of the C−C stretching and C−H bending modes (~2300 cm^{-1}), is not apparent for the H_2O−acetonitrile mixture.[50] Moreover, the C≡N stretch shows significant changes in the spectral shape and shifts in the central frequency at a different pH for the α-Al_2O_3(0001) and the SiO_2 surfaces in the PPP polarization combination.

To explore the effect of surface charge density, the aqueous component of the H_2O−acetonitrile mixture was pH-adjusted. For the α-Al_2O_3(0001) surface, the central frequency of the spectrum of the C≡N stretch is red-shifted at pH 10 and blue-shifted at pH 4 compared to pH 6. For the SiO_2 surface, the shifts in the nitrile mode as the pH increases from pH 6 to 9 to 12 are less obvious. At the α-Al_2O_3(0001)/H_2O−acetonitrile interface (Figure 1A), a symmetric spectral shape was observed at pH 4. As the pH is increased to 6, an asymmetric pattern emerges with higher magnitude at pH 10. On the other hand, as shown in Figure 1B, at the SiO_2/H_2O−acetonitrile interfaces, the C≡N stretch peak has a symmetric shape at pH 6. However, above pH 9, the vSFG response becomes asymmetric.

The C≡N stretch of acetonitrile (~2250 cm^{-1}) falls in the range where the relatively wide combination band of H_2O (bend + libration) appears.[51] We hypothesize that the asymmetric line shape observed in the PPP spectra is the interference between the C≡N stretch of acetonitrile and the H_2O combination band, not a nonresonant background (the details can be found in the Supporting Information).[52] Additionally, we observed an increase in amplitude in the range of ~2200−2300 cm^{-1} in neat H_2O solutions under basic

https://doi.org/10.1021/acs.jpcc.4c00306
J. Phys. Chem. C XXXX, XXX, XXX−XXX

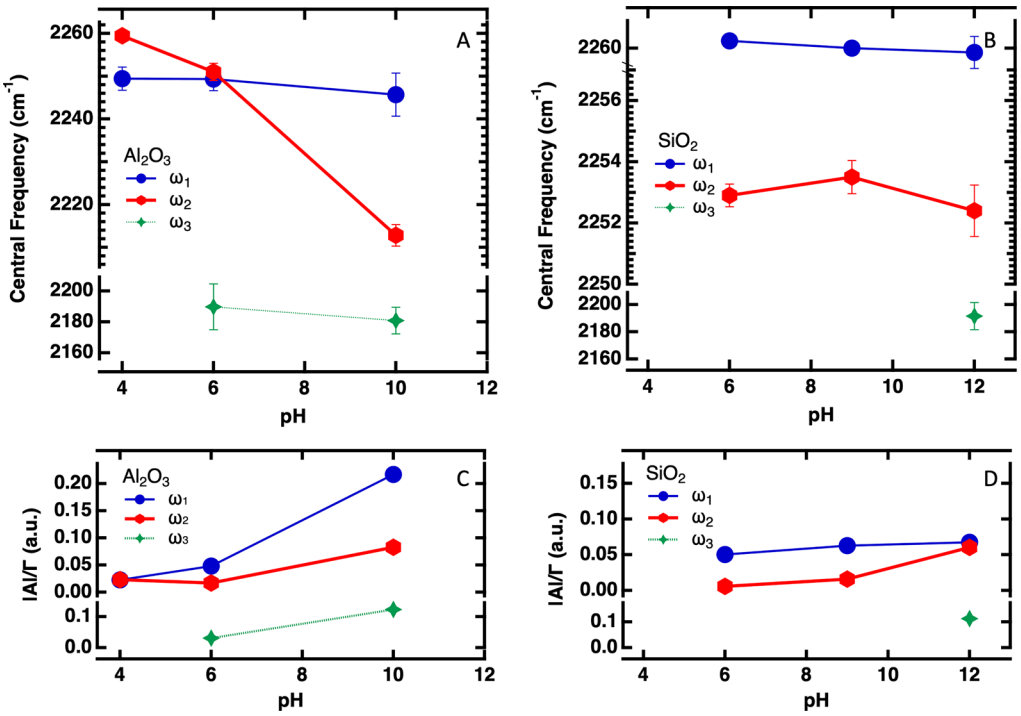

Figure 2. Fitting results of the normalized PPP vSFG data presented in Figure 1 using eq 1. The central frequency of the Lorentzian oscillators, with constant frequency (ω_1 blue), variable frequency (ω_2 red), and H_2O (ω_3 green) at the (A) α-Al_2O_3(0001) and (B) SiO_2 surfaces. The amplitude to line width ratio ($|A|/\Gamma$) of the C≡N stretch and the H_2O combination band (bend + libration) at the (C) α-Al_2O_3(0001) and (D) SiO_2 interfaces. The details and tabulated fit parameter values can be found in the Supporting Information, Tables S2.

conditions, suggesting a possible contribution from the H_2O combination band (Figure S2). To understand if this was the origin of the asymmetric line shapes observed in the vSFG of the H_2O−acetonitrile mixtures, we simulated the interaction of two Lorentzian oscillators with opposite amplitudes, one with a broader line width characteristic of the H_2O combination band and the other with a narrower line width for the C≡N stretch, Figure S3. The simulated results support the hypothesis that there is an interference between the C≡N stretch and the H_2O combination band Figure S3. We did not observe such asymmetric patterns for neat acetonitrile at either α-Al_2O_3(0001) or SiO_2 surfaces (Figure 1A,B: gray); further details can be found in the Supporting Information Figure S5. We tested the possibility of observing changes in the spectral shape at the PPP and SSP polarizations caused by Fresnel factor enhancement since the refractive index of the solvents is highly frequency-dependent.[53,54] We observed a relatively flat frequency-dependent Fresnel factor response at ∼2200−2300 cm^{-1}, as discussed in more detail in the Supporting Information, Figure S6. The absence of an asymmetric line shape in the vSFG response with neat acetonitrile and the lack of frequency dependence in the Fresnel factor response (Figure S6B,D), along with the intensity increase at the oxide interface with neat H_2O at higher pH, indicate that the interfacial H_2O combination band, rather than linear optical effects or a nonresonant response, contributes to the asymmetry of the vSFG response in the C≡N stretch region of aqueous acetonitrile solutions under basic conditions.

To quantitatively analyze the data, we fit the spectra for PPP and SSP polarization combinations using eq 1.

$$I(\omega_{\mathrm{vSFG}}) \propto |\chi^{(2)}_{\mathrm{eff}}|^2 I_{\mathrm{Vis}} I_{\mathrm{IR}} = \left|\chi^{(2)}_{\mathrm{NR}} e^{i\varphi_{\mathrm{NR}}} + \sum_{\nu} \chi^{(2)}_{\mathrm{R},\nu}\right|^2 I_{\mathrm{Vis}} I_{\mathrm{IR}} = \left|\chi^{(2)}_{\mathrm{NR}} e^{i\varphi_{\mathrm{NR}}} + \sum_{\nu} \frac{A_\nu}{\omega_{\mathrm{IR}} - \omega_\nu + i\Gamma_\nu}\right|^2 I_{\mathrm{Vis}} I_{\mathrm{IR}} \quad (1)$$

where the parameters are amplitude (A_ν), damping coefficient (Γ_ν), central frequency (ω_ν) of the νth vibrational mode, and phase (φ) between the second-order nonresonant ($\chi^{(2)}_{\mathrm{NR}}$) and resonant ($\chi^{(2)}_{\mathrm{R},\nu}$) nonlinear susceptibilities. Fitting of the spectra corresponding to the H_2O−acetonitrile mixture (Figure 1A,B) requires two Lorentzian oscillators for pH 4 [α-Al_2O_3(0001)] and pH 6 and 9 (SiO_2) and three Lorentzian oscillators for pH 6 and 10 [α-Al_2O_3(0001)] and pH 12 (SiO_2). Analysis of the fitting results from both surfaces suggests the presence of two distinct acetonitrile species. Given that the amplitudes do not consistently show opposite signs at both interfaces, we cannot assign the two species to the oppositely oriented inner and outer leaflets of a bilayer that have been reported for acetonitrile at water/silica interfaces.[16] We assigned the first species to have a constant central frequency, while the second species had a central frequency that varied depending on the surface charge. The oscillators with constant central frequency (ω_1) were the major contributors to the spectra, particularly at higher pH, which we attribute to acetonitrile interacting with hydroxyl groups, most of which are not charged even at higher pH (Figure 2A,B, blue). This is discussed in more detail below. For the silica system, which has been argued to lead to an acetonitrile bilayer interfacial structure,[16] it is possible that these acetonitrile molecules that contribute to ω_1 represent the outer leaflet directed away from the surface; previous studies have proposed that the outer leaflet of the acetonitrile bilayer

https://doi.org/10.1021/acs.jpcc.4c00306
J. Phys. Chem. C XXXX, XXX, XXX−XXX

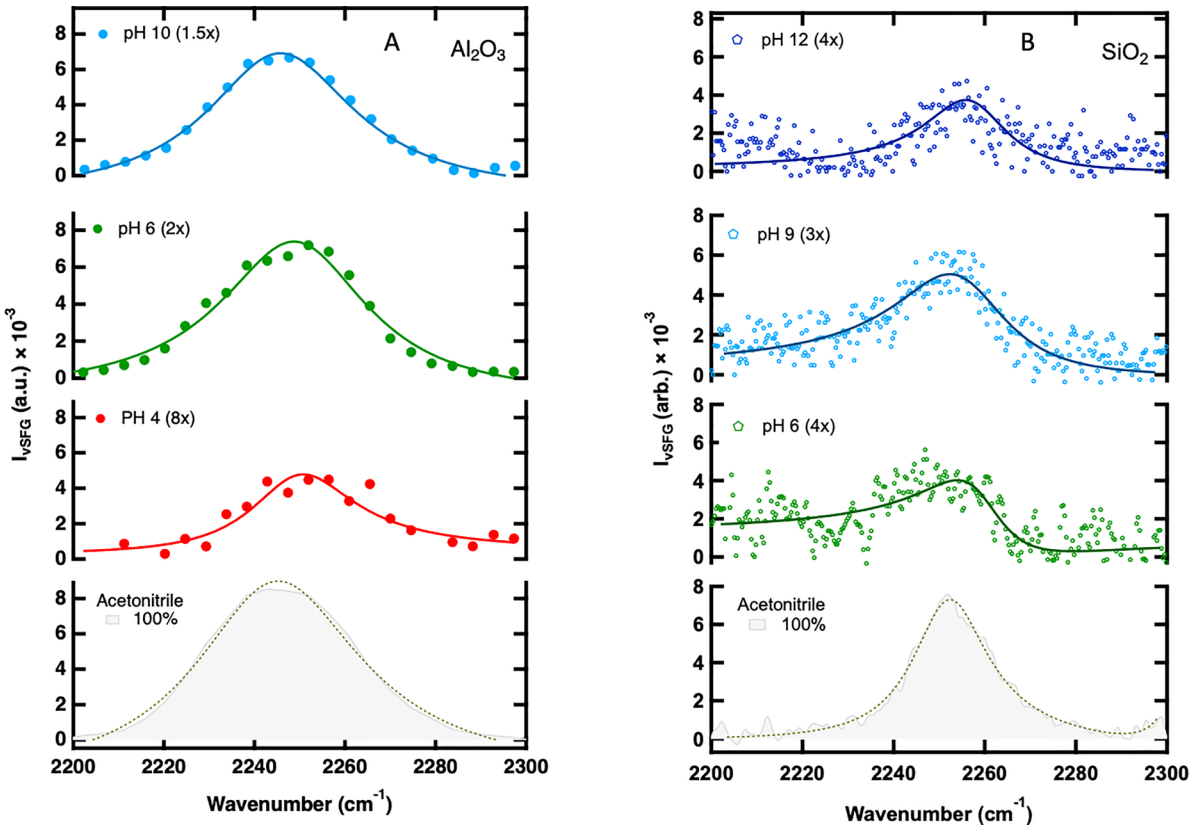

Figure 3. vSFG spectra of H_2O−acetonitrile solutions in the C≡N stretch region using the SSP polarization combination. (A) α-Al_2O_3(0001) interface at pH of 4, 6, and 10 and 100% acetonitrile and at the (B) SiO_2 interface at pH of 6, 9, and 12 and 100% acetonitrile. The vSFG spectra of the mixture for both surfaces and 100% acetonitrile at the α-Al_2O_3(0001) surface are fitted using one Lorentzian oscillator, while for the 100% acetonitrile at the SiO_2 surface, two Lorentzian functions are employed. The details and tabulated fit parameter values can be found in the Supporting Information, Tables S1 and S3. The response for 100% acetonitrile is shown in gray at the bottom of each panel.

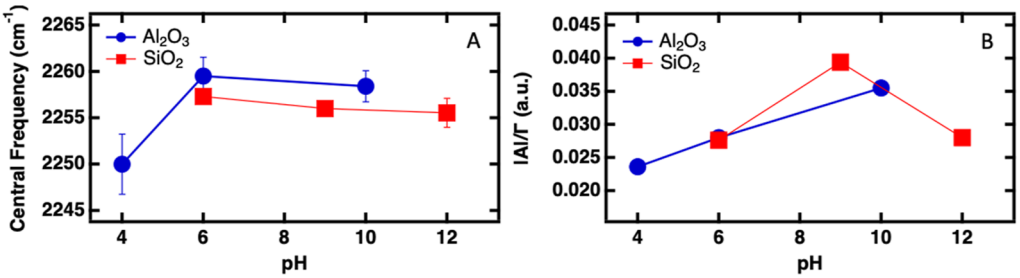

Figure 4. Fitting results of the normalized SSP vSFG data shown in Figure 3 using eq 1; (A) central frequency of the Lorentzian oscillators at the α-Al_2O_3(0001) and SiO_2 surfaces and (B) amplitude and line width ratio ($|A_i|/\Gamma_i$) of the C≡N stretch at the α-Al_2O_3(0001) and SiO_2 surfaces. vSFG spectra are fit using one Lorentzian function for the SSP polarization combination. The details and tabulated fit parameter values can be found in the Supporting Information, Table S3.

contributes most to the vSFG spectra.[16] However, such a bilayer structure is unknown for alumina. The oscillators whose central frequencies (ω_2) were affected by surface charge were minor contributors (Figure 2A,B, red). The ω_2 at the α-Al_2O_3(0001) red-shifts (~37 cm^{-1}) at pH 10 and blue-shifts (~10 cm^{-1}) at pH 4 relative to pH 6. For the SiO_2 surface, ω_2 red-shifts (~7 in average cm^{-1}) upon increasing the pH from 6 to 9 and 12 with respect to the constant frequency, ω_1. In contrast to our observation of a significant change in the central frequency of the C≡N stretch attributed to the ω_2 mode at both oxide interfaces, no shift was observed at the electrolyte/metal electrode interface with respect to the surface potential.[43] Finally, the extracted width of the third oscillator (Γ_3 ~ 100−200 cm^{-1} and much broader compared to the C≡N stretch) led us to consider its identity as the H_2O combination band (Figure 2A,B, green).[51] Consistent with this assignment, we observed an increase in the intensity in this region of the spectrum in the absence of acetonitrile (for the silica/neat H_2O interface) upon increasing the pH (Figure S2). The H_2O combination band (bend + libration: ~ 2000−2300 cm^{-1}) has been studied in the bulk using IR and Raman spectroscopies and proposed to be a sensitive probe of the hydrogen-bonding environment of bulk water without the contribution of the Fermi resonance that complicates the O−H stretch region.[51,55] However, attempts to detect the H_2O combination band (bend + libration) at interfaces using vSFG have not been successful.[56] We proposed that the interference with another mode, as reported here, can be an approach to

https://doi.org/10.1021/acs.jpcc.4c00306
J. Phys. Chem. C XXXX, XXX, XXX−XXX

access this band. The tabulated fit parameters for the pure acetonitrile and H_2O−acetonitrile mixture can be found in the Supporting Information, Tables S1−S3.

In contrast to the PPP polarization, the SSP polarization combination reveals a consistently symmetric vSFG response for the nitrile mode at all pH values for both interfaces (Figure 3A,B). Moreover, there is no significant shift in the central frequency versus the pH of the bulk solvents compared to the PPP response. The amplitudes of the vSFG responses at SSP and PPP polarization exhibit a consistent pattern, with higher intensity observed on surfaces with more negative charges. It is worth noting that the difference in the full-width half-maxima in both interfaces could be attributed to variation in the spectral resolution of the setups.

Unlike the PPP vSFG spectra (Figure 1A,B), we did not observe any asymmetry or frequency shift for the SSP polarization combination where a single Lorentzian oscillator was sufficient to fit the spectra (Figure 3A,B). The SSP nitrile mode shows almost no shift (Figure 4A) compared to the PPP polarization (Figure 2A,B). The acetonitrile species probed by the SSP polarization combination appear to have less sensitivity to the charged sites at the interfaces. It has been demonstrated that the CN frequency of acetonitrile molecules becomes less sensitive to electrode potentials as the molecules tilt away from normal incidence.[57] Thus, the central frequency of the CN peak shows no change when the molecule is lying flat to the surface, i.e., when the CN bond is perpendicular to the electric field. Therefore, we can argue that the acetonitrile molecules probed in the SSP polarization combination do not significantly respond to the electric field.

The contribution of net-oriented molecules at the interface can be described using the ratio of the amplitude and the line width ($|A_i|/\Gamma_i$) since $\chi_R^{(2)}$ is proportional to $|A_i|/\Gamma_i$ (eq 1). For the PPP polarization, the $|A_i|/\Gamma_i$ ratios for the C≡N stretch (ω_1, ω_2) and the H_2O combination band (ω_3) increase as the α-Al_2O_3(0001) becomes more negatively charged (Figure 2C). For the PPP vSFG response of the silica interface, the ω_3 mode becomes prominent at pH 12, making it difficult to resolve the subtle changes in $|A_i|/\Gamma_i$ of ω_1 and ω_2 (Figure 2D). For the SSP spectra where only one C≡N oscillator dominated, $|A_i|/\Gamma_i$ was nonmonotonic at the SiO_2 surface with increasing pH (Figure 4B). The decrease in $|A_i|/\Gamma_i$ at high pH is consistent with previous work monitoring the methyl vibrational modes of acetonitrile at the silica/aqueous interface, where we proposed that the acetonitrile was depleted from the interface owing to the more negatively charged silica.[16] In contrast, $|A_i|/\Gamma_i$ linearly increased at the α-Al_2O_3(0001) surfaces versus bulk pH similar to that observed for the PPP polarization (Figure 2C).

As the α-Al_2O_3(0001)/H_2O−acetonitrile interface becomes negatively charged, the $|A_i|/\Gamma_i$ of the C≡N ω_1 stretch increases and the H_2O combination band (bend + libration) appears above pH 6 (Figures 1A and 2C). At the positively charged α-Al_2O_3(0001) surface (at pH 4, some terminal hydroxyl groups are protonated to Al−OH^{2+}),[58] we hypothesize that the acetonitrile molecules that dominate the surface vSFG response are oriented with the −C≡N polar head (partially negatively charged) directed toward the oxide surface based on the observations of acetonitrile at positively charged metal surfaces.[43,45] This orientation would direct the hydrophobic $-CH_3$ predominantly toward the bulk H_2O,[43,45] which we propose leads to fewer H_2O molecules oriented in the interfacial region. The absence of the H_2O combination band (bend + libration) (ω_3) at the positively charged surface compared to the negatively charged surface supports this hypothesis (Figure 2C). Yet we note that we expected to see more net-oriented H_2O molecules at the positively charged α-Al_2O_3(0001) surface compared to the neutral surface based on observations for the alumina/H_2O interface,[59] which could suggest that the H_2O combination band is sensitive to the net orientation of H_2O or that the acetonitrile minimizes H_2O ordering at the positive surface.

At the negatively charged surface, we hypothesize that the CH_3 headgroup would direct toward the oxide surface.[43,45] At the α-Al_2O_3(0001) surface, due to the presence of a higher density of surface OH groups (~15 OH groups/nm^2) compared to the SiO_2 (~5 OH groups/nm^2) and greater surface charge (Al_2O_3:13 $\mu C/cm^2$ at pH 10 compared to SiO_2: 4.5 $\mu C/cm^2$ at pH 9), we expect to observe a higher population of the net-oriented acetonitrile and H_2O molecules in the interfacial region.[21,22,24,60] This hypothesis is supported by our results. For example, $|A_i|/\Gamma_i$ for all the interfacial species for pH 10 at the α-Al_2O_3(0001) has a higher value compared to the SiO_2 surface at pH 9 (Figure 2C,D). Unlike the positively charged surface, we propose that at the negatively charged alumina surface the polar −C≡N will attract and help to align the H_2O molecules in the interfacial region leading to a contribution from the H_2O combination band. Previous work has shown that for negatively charged α-Al_2O_3(0001), the vSFG response of the OH stretch (2800−3800 cm^{-1}) is higher compared to neutral surfaces as a result of a higher population of net-oriented H_2O molecules.[16,59] The presence of the combination band at pH 12 for the silica interface is also consistent with earlier work where the amount of oriented H_2O based on the vSFG response in the OH stretching region increased sharply between pH 9 and 12 for the silica interface in the presence of an aqueous acetonitrile solution (Figure 2D).[16]

The PPP and SSP polarizations can be used to extract information regarding the orientation of the transition dipole moment of the C≡N stretch of acetonitrile at both interfaces (the details can be found in the Supporting Information).[54] On the positively charged α-Al_2O_3(0001) surface, the angle of the molecular axis with respect to the surface normal is largest 66 ± 3° (Table 1); we assume that this corresponds to a net orientation away from the surface normal owing to the positive charged surface. At pH 6, the tilt angle of acetonitrile at the α-Al_2O_3(0001) decreases to 46 ± 3°, while the SiO_2 surface

Table 1. Tilt Angle of the Acetonitrile Molecule; Schematic Definition of the Tilt Angle Range (Black Wedge) from the Surface Normal (Vertical Black Arrow) Is Shown on the Right-Hand Side of the Table, at the SiO_2 and α-Al_2O_3(0001) Interfaces Determined UsingEq S6. Error Bars Have Been Determined by Using Multiple Sets of Data

Interface	pH	Tilt angle
α-Al_2O_3(0001)/ H_2O-acetonitrile	4	66° ± 3°
	6	46° ± 3°
	10	39°± 7°
α-Al_2O_3(0001)/ acetonitrile	neat	43° ± 2°
SiO_2/ H_2O-acetonitrile	6	31° ± 2°
	9	30 ± 1°
	12	5 ± 3°
SiO_2/acetonitrile	neat	47° ± 3°

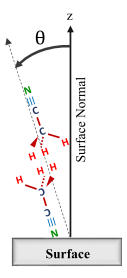

https://doi.org/10.1021/acs.jpcc.4c00306
J. Phys. Chem. C XXXX, XXX, XXX−XXX

exhibits an angle of 31 ± 2° with respect to the surface normal. As the surface becomes more negatively charged, the acetonitrile species probing the neutral sites orients more toward the surface normal (Table 1). Our results demonstrate that the average tilt angle of the net-oriented acetonitrile molecules, which appear to probe the neutral sites at both interfaces, is to some extent surface charge-dependent. Tilt angle analysis of acetonitrile molecules probing the charged sites (ω_2) is not feasible, as it necessitates $|A_i|/\Gamma_i$ for both PPP and SSP polarizations. While we detect SSP and PPP signals for neutral sites, the SSP response of the acetonitrile probing the charged sites is not as discernible, as a single Lorentzian suffices to fit the spectra.

VSES has utilized a range of nitrile and carbonyl probes as electric field reporters.[41,61] However, nitrile (−C≡N) probes have a relatively strong absorption coefficient and, unlike carbonyl (−CO), are in an IR spectral region uncluttered by strong water modes.[40] Our previous work using SCN^- as a probe molecule at neutral pH revealed a species ∼60 cm^{-1} blue-shifted with respect to ions experiencing neutral sites, which was attributed to K^+ SCN^- contact ion pairs at the interface.[1] However, in this study, we did not observe a shift of the C≡N stretch compared to its bulk value (∼2250 cm^{-1}) at the neutral α-Al_2O_3(0001) which corresponds to an average electric field of 0 MV/cm. In our previous work, we quantified the local electrostatic potential associated with the charged aluminol groups using 65 cm^{-1}/V Stark tuning corresponding to an externally applied bias across a platinum electrode.[1] Unlike SCN^-, for acetonitrile, only one study reported the Stark shifts of the C≡N vibration of the adsorbed acetonitrile molecules on a gold electrode to be around 4 cm^{-1}/V.[44]

To quantify the local electric field at the heterogeneously distributed charged sites associated with the charged hydroxyl groups at the α-Al_2O_3(0001) and the SiO_2 surfaces, we use this reported Stark tuning rate of 0.44 cm^{-1}/(MV/cm) for the C≡N stretch of bulk solution of acetonitrile[62,63] while tracking the spatially heterogeneous development of the localized surface charge by modulating the pH of the bulk solution. The vSFG spectra at PPP polarization reveal the existence of two types of acetonitrile species at the interface, with the central frequency of one of the oscillators being dependent on the surface charge. Hence, it appears that one acetonitrile species probes the neutral sites (or is oriented away from the interface) and the other probes the charged sites at the α-Al_2O_3(0001) and the SiO_2 interfaces.

The impact of an external electric field on vibrational frequency of an oscillator (linear vibrational Stark effect) can be calculated using eq 2.

$$\omega - \omega_0 \approx \Delta\mu \cdot F_{ext} \quad (2)$$

where ω and ω_0 are the frequencies at the applied and zero electric field, respectively, $\Delta\mu$ is the Stark tuning rate expressed in the units of cm^{-1}/(MV/cm), and F_{ext} is the applied external electric field.[40,41,64,65]

The Stark effect sensitivity of the C≡N stretch of acetonitrile gives us an opportunity to measure the local electric field.[41] The constant frequency oscillators (ω_1) are the major contributors at each pH and serve as a reference frequency for 0 MV/cm electric field (Figure 2A,B). At the positively and the negatively charged α-Al_2O_3(0001) surfaces, the variable frequency oscillators (ω_2) experienced a shift of ∼+10 and ∼−36 cm^{-1} with respect to the constant frequency oscillator at 2250 cm^{-1}, respectively. This corresponds to a local electric field of 4.3 MV/cm, 0 MV/cm, and −16 MV/cm at the positively, neutral, and negatively charged sites of the α-Al_2O_3(0001) surface, respectively (Figure 5). At pH 6, the SiO_2 surface is negatively charged (PZC ∼ pH 2−4) and by increasing the pH from 6 to 9 to 12, the oscillators with variable central frequency (ω_2) experienced a shift of ∼7 cm^{-1} compared to the reference frequency at 2260 cm^{-1}. This shift corresponds to electric fields of −3.2, −3.0, and −3.4 MV/cm experienced by acetonitrile at the SiO_2 surface, respectively (Figure 5). This value is in the ballpark for the average static electric field present in the Stern layer at pH 10 with 10 mM NaCl electrolyte in the absence of acetonitrile (−4.1 MV/cm, vide supra; the details can be found in the Supporting Information).[31] Yet surface potential and zeta potential measurements at aqueous silica interfaces exhibit significant pH dependence over this pH range from pH 6 and 9 and above.[30] The spectral shift observed here suggests that the acetonitrile molecules that sample the static electric field emanating from the silica surface only experience single negative sites even at pH 12.

The increased electric field and corresponding larger Stark shift at the α-Al_2O_3(0001) compared to the SiO_2 surface are likely due to the higher density of charged hydroxyl sites. Using potentiometric titration data for the α-Al_2O_3(0001) and SiO_2 surfaces, along with the number of hydroxyl groups present on each surface, it can be inferred that if every charged site produces 1 elementary charge, then at pH 10, approximately 1 out of 15 groups/nm^2 and 0.5 out of 5 hydroxyl groups/nm^2 are deprotonated, respectively.[21,60,66] The higher density of deprotonated sites for α-Al_2O_3(0001) is consistent with our observation of a greater shift for the negatively charged alumina (pH 10: ∼36 cm^{-1}) compared to SiO_2 (pH 6−12: ∼7 cm^{-1}).

For alumina, the magnitude of the electric field differs between the positively charged (4.3 MV/cm) and the negatively charged (−16 MV/cm) alumina surfaces. The measured value for the positively charged site is in close agreement with the calculated value (eq S6: electric field for a point charge), 3.9 MV/cm (Table S6). For the negatively charged sites, the measured value exceeds the calculated value by 4.8 MV/cm. One possible explanation is that individual acetonitrile molecules that exhibit pH-dependent frequencies at the alumina interface experience several local charged sites at

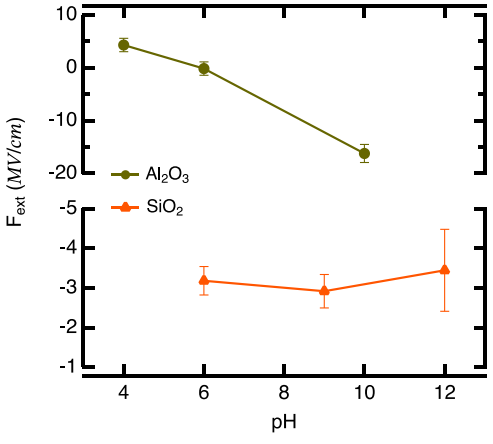

Figure 5. Calculated local electric field probed by acetonitrile in H_2O/acetonitrile mixtures at the α-Al_2O_3(0001) and the SiO_2 surfaces versus bulk pH.

https://doi.org/10.1021/acs.jpcc.4c00306
J. Phys. Chem. C XXXX, XXX, XXX−XXX

high pH. However, we would anticipate that the nitrile frequency of acetonitrile probing the neutral sites should also be influenced. Nevertheless, the presence of ordered H_2O molecules which could potentially replace acetonitrile at these neutral sites may explain why we do not observe a shift in their frequency, as the acetonitrile molecules do not interact with the neutral sites. Another contributing factor could be the increased number of acetonitrile molecules oriented toward the bulk, which interact with ordered H_2O molecules near the interface through weak hydrogen bonding between the C≡N and OH groups, rather than with neutral hydroxyl sites. The prior CH stretch study revealed an increased density of oriented H_2O molecules replacing acetonitrile molecules on negatively charged surfaces, reflecting similar findings on SiO_2 surfaces.[16] Rehl et al. attributed this to the instability of acetonitrile bilayers or the deprotonation of silanol groups to create siloxides, which ultimately results in heightened H_2O solvation of the surface sites and the displacement of acetonitrile that was originally bonded with or near the SiOH groups.[16] This reason could not apply for the positively charged sites on the Al_2O_3 surface as the C≡N head orients toward the surface and not the bulk, and we do not observe net-oriented H_2O molecules based on the absence of the H_2O combination band feature. We conclude that the charge of the hydroxyl groups at the interface can affect the orientation of the probe molecules at the interface, consequently influencing the magnitude of the electric field.

CONCLUSIONS

The molecular arrangement and local electric fields experienced by the first few layers of H_2O−acetonitrile mixtures at the α-Al_2O_3(0001) and SiO_2 surfaces were investigated as a function of the surface charge using vSFG spectroscopy. An asymmetric line shape was observed under basic conditions that was attributed to interference between the H_2O combination (bend + libration) band and the nitrile stretch. We propose that the presence of this H_2O combination band is correlated with the presence of oriented H_2O due to the interfacial polar nitrile group. At low pH values where the α-Al_2O_3(0001) surface is positively charged, the polar −C≡N head of acetonitrile is expected to be directed toward the surface, which we suggest leads to no combination band owing to a smaller population of net-oriented H_2O in the interfacial region due to hydrophobic interactions with the $-CH_3$ groups. Under conditions where the surfaces are negative, the amount of ordered H_2O appears to increase with increasing pH based on the growing amplitude of the H_2O combination band.

After accounting for the interference in our spectral fitting, we carried out vibrational Stark spectroscopy of the nitrile stretch and found that α-Al_2O_3 has a greater local electric field than SiO_2 (−16 MV/cm *vs* ∼−3 MV/cm) at higher pH (pH 10 and 9−12, respectively). This significant difference in the magnitude of the electric field at these negatively charged oxides is attributed to a higher density of charged hydroxyl groups at the α-Al_2O_3(0001) compared to the SiO_2 surface. Furthermore, the electric field at pH 10 for the alumina interface is significantly greater than what would be expected from a single negative site indicating that the acetonitrile experiences local fields that are additive based on the close proximity of multiple charged sites. In contrast, we observe a pH-independent local electric field for the silica interface at pH 6, 9, and 12, which all correspond to net negatively charged surfaces albeit with different expected surface charge densities and interfacial potentials. These results suggest that the local electric fields near a negative site are independent of pH until a certain charge density is reached, whereby the electric fields emanating from multiple sites overlap.

ASSOCIATED CONTENT

Supporting Information

The Supporting Information is available free of charge at https://pubs.acs.org/doi/10.1021/acs.jpcc.4c00306.

Detailed description of experimental procedures, arguments supporting the observation of the combination band of H_2O (bend + libration) through interference with the C≡N stretch of acetonitrile, tabulated extracted fit parameters for all systems at both PPP and SSP polarization, Fresnel factor correction for the mixtures, orientational analysis, and surface charge sites and average electric field calculations (PDF)

AUTHOR INFORMATION

Corresponding Authors

Julianne M. Gibbs − *Department of Chemistry, University of Alberta, Edmonton, Alberta T6G 2G2, Canada;* orcid.org/0000-0001-5819-2306; Email: julianne.gibbs@ualberta.ca

Eric Borguet − *Department of Chemistry, Temple University, Philadelphia, Pennsylvania 19122, United States;* orcid.org/0000-0003-0593-952X; Email: eborguet@temple.edu

Authors

Somaiyeh Dadashi − *Department of Chemistry, Temple University, Philadelphia, Pennsylvania 19122, United States;* orcid.org/0009-0003-3249-3428

Shyam Parshotam − *Department of Chemistry, University of Alberta, Edmonton, Alberta T6G 2G2, Canada;* orcid.org/0000-0002-5890-4411

Bijoya Mandal − *Department of Chemistry, Temple University, Philadelphia, Pennsylvania 19122, United States*

Benjamin Rehl − *Department of Chemistry, University of Alberta, Edmonton, Alberta T6G 2G2, Canada;* orcid.org/0000-0002-5534-6717

Complete contact information is available at: https://pubs.acs.org/10.1021/acs.jpcc.4c00306

Notes

The authors declare no competing financial interest.

ACKNOWLEDGMENTS

E.B. thanks the National Science Foundation (CHE 2102557) for supporting this work. The authors also thank Professor M. Zdilla (Temple University, Chemistry Department) for α-Al_2O_3(0001) prism face orientation identification via X-ray diffraction and Dr. Kyle Gilroy (Professor S. Neretina group, Temple University, College of Engineering) for gold-coating α-Al_2O_3(0001) prisms that were used for vSFG data normalization. J.M.G. thanks the Natural Sciences and Engineering Research Council of Canada for financial support (Discovery Grant).

REFERENCES

(1) Beć, K. B.; Grabska, J.; Huck, C. W. Near-Infrared Spectroscopy in Bio-Applications. *Molecules* **2020**, *25*, 2948.

(2) Henry, M. C.; Piagessi, E. A.; Zesotarski, J. C.; Messmer, M. C. Sum-Frequency Observation of Solvent Structure at Model Chromatographic Interfaces: Acetonitrile-Water and Methanol-Water Systems. *Langmuir* **2005**, *21*, 6521−6526.
(3) Saitoh, T.; Nakayama, Y.; Hiraide, M. Concentration of Chlorophenols in Water with Sodium Dodecylsulfate -γ-Alumina Admicelles for High-Performance Liquid Chromatographic Analysis. *J. Chromatogr. A* **2002**, *972*, 205−209.
(4) Laurent, C.; Billiet, H. A. H.; de Galan, L. On the Use of Alumina in HPLC with Aqueous Mobile Phases at Extreme pH. *Chromatographia* **1983**, *17*, 253−258.
(5) Kirkland, J. J.; Henderson, J. W.; DeStefano, J. J.; Van Straten, M. A.; Claessens, H. A. Stability of Silica-Based, Endcapped Columns with pH 7 and 11 Mobile Phases for Reversed-Phase High-Performance Liquid Chromatography. *J. Chromatogr. A* **1997**, *762*, 97−112.
(6) Mao, Y.; Fung, B. M. Use of Alumina with Anchored Polymer Coating as Packing Material for Reversed-Phase High-Performance Liquid Chromatography. *J. Chromatogr. A* **1997**, *790*, 9−15.
(7) Hemström, P.; Irgum, K. Hydrophilic Interaction Chromatography. *J. Sep. Sci.* **2006**, *29*, 1784−1821.
(8) Buszewski, B.; Noga, S. Hydrophilic Interaction Liquid Chromatography (HILIC)-a Powerful Separation Technique. *Anal. Bioanal. Chem.* **2012**, *402*, 231−247.
(9) Steinrück, H. G.; Cao, C.; Tsao, Y.; Takacs, C. J.; Konovalov, O.; Vatamanu, J.; Borodin, O.; Toney, M. F. The Nanoscale Structure of the Electrolyte-Metal Oxide Interface. *Energy Environ. Sci.* **2018**, *11*, 594−602.
(10) Huang, J.; Climent, V.; Groß, A.; Feliu, J. M. Understanding Surface Charge Effects in Electrocatalysis. Part 2: Hydrogen Peroxide Reactions at Platinum. *Chin. J. Catal.* **2022**, *43*, 2837−2849.
(11) Rivera, C. A.; Bender, J. S.; Manfred, K.; Fourkas, J. T. Persistence of Acetonitrile Bilayers at the Interface of Acetonitrile/Water Mixtures with Silica. *J. Phys. Chem. A* **2013**, *117*, 12060−12066.
(12) Liu, S.; Hu, Z.; Weeks, J. D.; Fourkas, J. T. Structure of Liquid Propionitrile at Interfaces. 1. Molecular Dynamics Simulations. *J. Phys. Chem. C* **2012**, *116*, 4012−4018.
(13) Tadjeddine, A.; Guyot-Sionnest, P. Spectroscopic Investigation of Adsorbed Cyanide and Thiocyanate on Platinum Using Sum Frequency Generation. *Electrochim. Acta* **1991**, *36*, 1849−1854.
(14) Zhang, D.; Gutow, J. H.; Eisenthal, K. B.; Heinz, T. F. Sudden Structural Change at an Air/Binary Liquid Interface: Sum Frequency Study of the Air/Acetonitrile-Water Interface. *J. Chem. Phys.* **1993**, *98*, 5099−5101.
(15) Berne, B. J.; Fourkas, J. T.; Walker, R. A.; Weeks, J. D. Nitriles at Silica Interfaces Resemble Supported Lipid Bilayers. *Acc. Chem. Res.* **2016**, *49*, 1605−1613.
(16) Rehl, B.; Li, Z.; Gibbs, J. M. Influence of High pH on the Organization of Acetonitrile at the Silica/Water Interface Studied by Sum Frequency Generation Spectroscopy. *Langmuir* **2018**, *34*, 4445−4454.
(17) Kim, J.; Chou, K. C.; Somorjai, G. A. Structure and Dynamics of Acetonitrile at the Air/Liquid Interface of Binary Solutions Studied by Infrared-Visible Sum Frequency Generation. *J. Phys. Chem. B* **2003**, *107*, 1592−1596.
(18) Bañuelos, J. L.; Borguet, E.; Brown, G. E.; Cygan, R. T.; Deyoreo, J. J.; Dove, P. M.; Gaigeot, M. P.; Geiger, F. M.; Gibbs, J. M.; Grassian, V. H.; et al. Oxide- and Silicate-Water Interfaces and Their Roles in Technology and the Environment. *Chem. Rev.* **2023**, *123*, 6413−6544.
(19) Kosmulski, M. The pH Dependent Surface Charging and Points of Zero Charge. IX. Update. *Adv. Colloid Interface Sci.* **2021**, *296*, 102519.
(20) Zhang, L.; Tian, C.; Waychunas, G. A.; Shen, Y. R. Structures and Charging of α-Alumina (0001)/Water Interfaces Studied by Sum-Frequency Vibrational Spectroscopy. *J. Am. Chem. Soc.* **2008**, *130*, 7686−7694.
(21) Ntalikwa, J. W. Determination of Surface Charge Density of α-Alumina by Acid−Base Titration. *Bull. Chem. Soc. Ethiop.* **2007**, *21*, 117−128.
(22) Chen, J.; Sharapa, D.; Plessow, P. N. Stability and Formation of Hydroxylated α-Al_2 O_3(0001) Surfaces at High Temperatures. *Phys. Rev. Res.* **2022**, *4*, 013232.
(23) Ong, S.; Zhao, X.; Eisenthal, K. B. Polarization of Water Molecules at a Charged Interface: Second Harmonic Studies of the Silica/Water Interface. *Chem. Phys. Lett.* **1992**, *191*, 327−335.
(24) Schrader, A. M.; Monroe, J. I.; Sheil, R.; Dobbs, H. A.; Keller, T. J.; Li, Y.; Jain, S.; Shell, M. S.; Israelachvili, J. N.; Han, S. Surface Chemical Heterogeneity Modulates Silica Surface Hydration. *Proc. Natl. Acad. Sci. U.S.A.* **2018**, *115*, 2890−2895.
(25) Sulpizi, M.; Gaigeot, M.-P.; Sprik, M. The Silica-Water Interface: How the Silanols Determine the Surface Acidity and Modulate the Water Properties. *J. Chem. Theory Comput.* **2012**, *8*, 1037−1047.
(26) Azam, S.; Darlington, A.; Gibbs-Davis, J. M. The Influence of Concentration on Specific Ion Effects at the Silica/Water Interface. *J. Phys.: Condens. Matter* **2014**, *26*, 244107.
(27) Darlington, A. M.; Gibbs-Davis, J. M. Bimodal or Trimodal? The Influence of Starting pH on Site Identity and Distribution at the Low Salt Aqueous/Silica Interface. *J. Phys. Chem. C* **2015**, *119*, 16560−16567.
(28) Gaigeot, M. P.; Sprik, M.; Sulpizi, M. Oxide/Water Interfaces: How the Surface Chemistry Modifies Interfacial Water Properties. *J. Phys.: Condens. Matter* **2012**, *24*, 124106.
(29) Contescu, C.; Jagiełło, J.; Schwarz, J. A. Heterogeneity of Proton Binding Sites at the Oxide/Solution Interface. *Langmuir* **1993**, *9*, 1754−1765.
(30) Rehl, B.; Ma, E.; Parshotam, S.; Dewalt-Kerian, E. L.; Liu, T.; Geiger, F. M.; Gibbs, J. M. Water Structure in the Electrical Double Layer and the Contributions to the Total Interfacial Potential at Different Surface Charge Densities. *J. Am. Chem. Soc.* **2022**, *144*, 16338−16349.
(31) Brown, M. A.; Goel, A.; Abbas, Z. Effect of Electrolyte Concentration on the Stern Layer Thickness at a Charged Interface. *Angew. Chem., Int. Ed.* **2016**, *55*, 3790−3794.
(32) Delon, T.; Parsai, T.; Kilic, U.; Schubert, M.; Morin, S. A.; Li, Y. Impacts of Particle Surface Heterogeneity on the Deposition of Colloids on Flat Surfaces. *Environ. Sci. Nano* **2021**, *8*, 3365−3375.
(33) Piontek, S. M.; Dellostritto, M.; Mandal, B.; Marshall, T.; Klein, M. L.; Borguet, E. Probing Heterogeneous Charge Distributions at the α-Al_2O_3(0001)/H_2O Interface. *J. Am. Chem. Soc.* **2020**, *142*, 12096−12105.
(34) Bagchi, S.; Fried, S. D.; Boxer, S. G. A Solvatochromic Model Calibrates Nitriles' Vibrational Frequencies to Electrostatic Fields. *J. Am. Chem. Soc.* **2012**, *134*, 10373−10376.
(35) Suydam, I. T.; Snow, C. D.; Pande, V. S.; Boxer, S. G. Electric Fields at the Active Site of an Enzyme: Direct Comparison of Experiment with Theory. *Science* **2006**, *313*, 200−204.
(36) Wang, L.; Fried, S. D.; Boxer, S. G.; Markland, T. E. Quantum Delocalization of Protons in the Hydrogen-Bond Network of an Enzyme Active Site. *Proc. Natl. Acad. Sci. U.S.A.* **2014**, *111*, 18454−18459.
(37) Fried, S. D.; Boxer, S. G. Electric Fields and Enzyme Catalysis. *Annu. Rev. Biochem.* **2017**, *86*, 387−415.
(38) Baldelli, S. Probing Electric Fields at the Ionic Liquid-Electrode Interface Using Sum Frequency Generation Spectroscopy and Electrochemistry. *J. Phys. Chem. B* **2005**, *109*, 13049−13051.
(39) Sorenson, S. A.; Patrow, J. G.; Dawlaty, J. M. Solvation Reaction Field at the Interface Measured by Vibrational Sum Frequency Generation Spectroscopy. *J. Am. Chem. Soc.* **2017**, *139*, 2369−2378.
(40) Weaver, J. B.; Kozuch, J.; Kirsh, J. M.; Boxer, S. G. Nitrile Infrared Intensities Characterize Electric Fields and Hydrogen Bonding in Protic, Aprotic, and Protein Environments. *J. Am. Chem. Soc.* **2022**, *144*, 7562−7567.

https://doi.org/10.1021/acs.jpcc.4c00306
J. Phys. Chem. C XXXX, XXX, XXX−XXX

(41) Suydam, I. T.; Boxer, S. G. Vibrational Stark Effects Calibrate the Sensitivity of Vibrational Probes for Electric Fields in Proteins. *Biochemistry* **2003**, *42*, 12050−12055.
(42) Irish, D. E.; Hill, I. R.; Archambault, P.; Atkinson, G. F. Investigations of Electrode Surfaces in Acetonitrile Solutions Using Surface-Enhanced Raman Spectroscopy. *J. Solution Chem.* **1985**, *14*, 221−243.
(43) Sayama, A.; Nihonyanagi, S.; Ohshima, Y.; Tahara, T. In Situ Observation of the Potential-Dependent Structure of an Electrolyte/Electrode Interface by Heterodyne-Detected Vibrational Sum Frequency Generation. *Phys. Chem. Chem. Phys.* **2020**, *22*, 2580−2589.
(44) Reinsberg, P. H.; Baltruschat, H. Potential- and Cation-Dependent Adsorption of Acetonitrile on Gold Investigated via Surface Enhanced Infrared Absorption Spectroscopy. *Electrochim. Acta* **2020**, *334*, 135609.
(45) Baldelli, S.; Mailhot, G.; Ross, P. N.; Somorjai, G. A. Potential-Dependent Vibrational Spectroscopy of Solvent Molecules at the Pt(111) Electrode in a Water/Acetonitrile Mixture Studied by Sum Frequency Generation. *J. Am. Chem. Soc.* **2001**, *123*, 7697−7702.
(46) Piontek, S. M.; Borguet, E. Vibrational Spectroscopy of Geochemical Interfaces. *Surface Science Reports* **2023**, *78*, 100606.
(47) Liu, S.; Fourkas, J. T. Orientational Time Correlation Functions for Vibrational Sum-Frequency Generation. 1. Acetonitrile. *J. Phys. Chem. A* **2013**, *117*, 5853−5864.
(48) Ding, F.; Hu, Z.; Zhong, Q.; Manfred, K.; Gattass, R. R.; Brindza, M. R.; Fourkas, J. T.; Walker, R. A.; Weeks, J. D. Interfacial Organization of Acetonitrile: Simulation and Experiment. *J. Phys. Chem. C* **2010**, *114*, 17651−17659.
(49) Zhang, D.; Gutow, J. H.; Eisenthal, K. B. Structural Phase Transitions of Small Molecules at Air/Water Interfaces. *J. Chem. Soc., Faraday Trans.* **1996**, *92*, 539−543.
(50) Saß, M.; Lettenberger, M.; Laubereau, A. Orientation and Vibrational Relaxation of Acetonitrile at a Liquid: Solid Interface, Observed by Sum-Frequency Spectroscopy. *Chem. Phys. Lett.* **2002**, *356*, 284−290.
(51) Verma, P. K.; Kundu, A.; Puretz, M. S.; Dhoonmoon, C.; Chegwidden, O. S.; Londergan, C. H.; Cho, M. The Bend+Libration Combination Band Is an Intrinsic, Collective, and Strongly Solute-Dependent Reporter on the Hydrogen Bonding Network of Liquid Water. *J. Phys. Chem. B* **2018**, *122*, 2587−2599.
(52) Kuo, C. H.; Hochstrasser, R. M. Two Dimensional Infrared Spectroscopy and Relaxation of Aqueous Cyanide. *Chem. Phys.* **2007**, *341*, 21−28.
(53) Backus, E. H. G.; Garcia-Araez, N.; Bonn, M.; Bakker, H. J. On the Role of Fresnel Factors in Sum-Frequency Generation Spectroscopy of Metal-Water and Metal-Oxide-Water Interfaces. *J. Phys. Chem. C* **2012**, *116*, 23351−23361.
(54) Wang, L.; Nihonyanagi, S.; Inoue, K. I.; Nishikawa, K.; Morita, A.; Ye, S.; Tahara, T. Effect of Frequency-Dependent Fresnel Factor on the Vibrational Sum Frequency Generation Spectra for Liquid/Solid Interfaces. *J. Phys. Chem. C* **2019**, *123*, 15665−15673.
(55) Darlington, A. M.; Jarisz, T. A.; Dewalt-Kerian, E. L.; Roy, S.; Kim, S.; Azam, M. S.; Hore, D. K.; Gibbs, J. M. Separating the pH-Dependent Behavior of Water in the Stern and Diffuse Layers with Varying Salt Concentration. *J. Phys. Chem. C* **2017**, *121*, 20229−20241.
(56) Sengupta, S.; Moberg, D. R.; Paesani, F.; Tyrode, E. Neat Water-Vapor Interface: Proton Continuum and the Nonresonant Background. *J. Phys. Chem. Lett.* **2018**, *9*, 6744−6749.
(57) Lake, W. R.; Meng, J.; Dawlaty, J. M.; Lian, T.; Hammes-Schiffer, S. Electro-Inductive Effect Dominates Vibrational Frequency Shifts of Conjugated Probes on Gold Electrodes. *J. Am. Chem. Soc.* **2023**, *145*, 22548−22554.
(58) Zhang, L.; Tian, C.; Waychunas, G. A.; Shen, Y. R. Structures and Charging of α-Alumina (0001)/Water Interfaces Studied by Sum-Frequency Vibrational Spectroscopy. *J. Am. Chem. Soc.* **2008**, *130*, 7686−7694.
(59) Tuladhar, A.; Piontek, S. M.; Borguet, E. Insights on Interfacial Structure, Dynamics, and Proton Transfer from Ultrafast Vibrational Sum Frequency Generation Spectroscopy of the Alumina(0001)/Water Interface. *J. Phys. Chem. C* **2017**, *121*, 5168−5177.
(60) Bolt, G. H. Determination of the Charge Density of Silica Sols. *J. Phys. Chem.* **1957**, *61*, 1166−1169.
(61) Flores, S. C.; Kherb, J.; Konelick, N.; Chen, X.; Cremer, P. S. The Effects of Hofmeister Cations at Negatively Charged Hydrophilic Surfaces. *J. Phys. Chem. C* **2012**, *116*, 5730−5734.
(62) Ringer, A. L.; MacKerell, A. D. Calculation of the Vibrational Stark Effect Using a First-Principles Quantum Mechanical/Molecular Mechanical Approach. *J. Phys. Chem. Lett.* **2011**, *2*, 553−556.
(63) Andrews, S. S.; Boxer, S. G. Vibrational Stark Effects of Nitriles II. Physical Origins of Stark Effects from Experiment and Perturbation Models. *J. Phys. Chem. A* **2002**, *106*, 469−477.
(64) Ge, A.; Videla, P. E.; Lee, G. L.; Rudshteyn, B.; Song, J.; Kubiak, C. P.; Batista, V. S.; Lian, T. Interfacial Structure and Electric Field Probed by in Situ Electrochemical Vibrational Stark Effect Spectroscopy and Computational Modeling. *J. Phys. Chem. C* **2017**, *121*, 18674−18682.
(65) Fafarman, A. T.; Sigala, P. A.; Schwans, J. P.; Fenn, T. D.; Herschlag, D.; Boxer, S. G. Quantitative, Directional Measurement of Electric Field Heterogeneity in the Active Site of Ketosteroid Isomerase. *Proc. Natl. Acad. Sci. U.S.A.* **2012**, *109*, E299−E308.
(66) Brown, M. A.; Abbas, Z.; Kleibert, A.; Green, R. G.; Goel, A.; May, S.; Squires, T. M. Determination of Surface Potential and Electrical Double-Layer Structure at the Aqueous Electrolyte-Nanoparticle Interface. *Phys. Rev. X* **2016**, *6*, 011007.

https://doi.org/10.1021/acs.jpcc.4c00306
J. Phys. Chem. C XXXX, XXX, XXX−XXX